Journal of Experimental Botany, Vol. 71, No. 22 pp. 6907–6920, 2020
doi:10.1093/jxb/eraa410 Advance Access Publication 9 September 2020

RESEARCH PAPER

TOR mediates the autophagy response to altered nucleotide homeostasis in an RNase mutant

Zakayo Kazibwe[1], Junmarie Soto-Burgos[1], Gustavo C. MacIntosh[2] and Diane C Bassham[1,*]

[1] Department of Genetics, Development and Cell Biology, Iowa State University, Ames, IA 50011, USA
[2] Roy J. Carver Department of Biochemistry, Biophysics and Molecular Biology, Iowa State University, Ames, IA 50011, USA

* Correspondence: bassham@iastate.edu

Received 27 April 2020; Editorial decision 1 September 2020; Accepted 6 September 2020

Editor: Peter Bozhkov, Swedish University of Agricultural Sciences, Sweden

Abstract

The *Arabidopsis thaliana* T2 family endoribonuclease RNS2 localizes to the vacuole and functions in rRNA degradation. Loss of RNS2 activity impairs rRNA turnover and leads to constitutive autophagy, a process for degradation of cellular components. Autophagy is normally activated during environmental stress and is important for stress tolerance and homeostasis. Here we show that restoration of cytosolic purine nucleotide levels rescues the constitutive autophagy phenotype of *rns2-2* seedlings, whereas inhibition of purine synthesis induces autophagy in wild-type seedlings. *rns2-2* seedlings have reduced activity of the target of rapamycin (TOR) kinase complex, a negative regulator of autophagy, and this phenotype is rescued by addition of inosine to increase purine levels. Activation of TOR in *rns2-2* by exogenous auxin blocks the enhanced autophagy, indicating a possible involvement of the TOR signaling pathway in the activation of autophagy in the *rns2-2* mutant. Our data suggest a model in which loss of rRNA degradation in *rns2-2* leads to a reduction in cytoplasmic nucleotide concentrations, which in turn inhibits TOR activity, leading to activation of autophagy to restore homeostasis.

Keywords: Arabidopsis, autophagy, inosine, nucleotides, RNase, RNS2, rRNA, target of rapamycin (TOR).

Introduction

Ribosome biosynthesis is a substantial sink of cellular resources (Warner, 1999; Doerner, 2007). Degradation and recycling of ribosomal components at the end of their useful life is therefore critical for homeostasis and for maintaining substrate concentrations for protein and RNA synthesis. In eukaryotes, degradation of rRNA is effected primarily by RNases belonging to the RNase T2 family localized in lytic organelles, lysosomes in animals and vacuoles in plants and yeast (Haud *et al.*, 2011; Hillwig *et al.*, 2011; Huang *et al.*, 2015; Liu *et al.*, 2018). In *Arabidopsis thaliana*, at least a portion of rRNA decay occurs in the vacuole via the RNS2 RNase (Hillwig *et al.*, 2011) after uptake by autophagy-related transport or alternative pathways (Floyd *et al.*, 2015). RNS2, like other RNase T2 enzymes, is a single strand-specific endoribonuclease, and localizes to the vacuole and endoplasmic reticulum (Hillwig *et al.*, 2011; Floyd *et al.*, 2017). The vacuolar degradation of rRNA is proposed to be important in nucleotide homeostasis (Bassham and MacIntosh, 2017) and, therefore, the RNA degradation products within vacuoles need to be exported to the cytoplasm for re-use by

Abbreviations: 6-AZA, 6-azauridine; 2,6-DAP, 2,6-diaminopurine; ENT1, Equilibrative Nucleoside Transporter 1; 5-FU, 5-fluorouracil; LTX, lometrexol; MDC, monodansylcadaverine; 6-MP, 6-mercaptopurine; MS, Murashige and Skoog; MTX, methotrexate; NAA, 1-naphthaleneacetic acid; SnRK1, sucrose non-fermenting-1-related protein kinase 1; TOR, target of rapamycin; T6P, trehalose-6-phosphate.

the cells. Based on work on the equivalent enzyme in yeast, Rnyl (Huang *et al.*, 2015), Arabidopsis RNS2 may hydrolyze RNA to 3'-nucleoside monophosphate (NMP), followed by dephosphorylation by an as yet unidentified vacuolar nucleoside phosphatase. The resulting nucleosides are then transported to the cytoplasm by the tonoplast-localized Equilibrative Nucleoside Transporter 1 (ENT1) (Bernard *et al.*, 2011). In the cytoplasm, these nucleosides can be converted to nucleobases and used in primary metabolism.

Consistent with a role in rRNA degradation, in Arabidopsis plants lacking RNS2 (*rns2-2*), rRNAs have a longer half-life compared with that of wild-type plants, and the mutants accumulate RNA inside their vacuoles (Hillwig *et al.*, 2011; Floyd *et al.*, 2015). Similar RNA accumulation phenotypes are seen in animals and humans with defects in RNase T2 genes (Henneke *et al.*, 2009; Haud *et al.*, 2011; Liu *et al.*, 2018). In addition, *rns2-2* mutants have constitutive activation of the autophagy pathway (Hillwig *et al.*, 2011; Floyd *et al.*, 2015). Autophagy is a conserved pathway for the vacuolar degradation and recycling of cellular components, including organelles and macromolecules (Li and Vierstra, 2012; Liu and Bassham, 2012). It involves the formation of double membrane structures, termed autophagosomes, that engulf cytoplasmic cargo and eventually fuse with the vacuole, in which the engulfed components are degraded (Wang *et al.*, 2018). In plants grown under normal conditions, autophagy is active only at low basal levels, but it is up-regulated during senescence and under nutrient deficiency and environmental stress (Doelling *et al.*, 2002; Hanaoka *et al.*, 2002; Liu and Bassham, 2012). Bulk autophagy in plants has been well studied, and autophagy-mediated degradation of certain cell organelles, such as mitochondria (Li *et al.*, 2014), the endoplasmic reticulum (Liu *et al.*, 2012), chloroplasts (Izumi *et al.*, 2017), and ribosomes (Floyd *et al.*, 2015), has also been reported.

The reason for the constitutive autophagy in *rns2-2* mutants is unknown but could be due to potential disruptions in nucleotide homeostasis and decreased cytosolic nucleotide concentrations. Insight can be obtained from a mutant in *Caenorhabditis elegans* in which the loss of the T2 family endoribonuclease RNST-2 causes accumulation of rRNA inside lysosomes, and results in larval and embryonic development defects and shortened life span (Liu *et al.*, 2018). These defects are more severe in double mutants that are also defective in nucleotide *de novo* synthesis, and supplementation of the double mutants with pyrimidine nucleotides suppresses these defects. This suggests that the lysosomal degradation of rRNA by RNST-2 is necessary to maintain pyrimidine homeostasis during *C. elegans* embryogenesis, and that vacuolar/lysosomal RNases may be important in maintaining cellular nucleotide concentrations. This is also supported by analysis of gene expression profiles of Arabidopsis *rns2-2* mutants compared with wild-type plants, which revealed differential regulation of genes encoding enzymes of the pentose phosphate pathway (PPP) (Morriss *et al.*, 2017). Additionally, the levels of PPP intermediates were significantly reduced in *rns2-2*, suggesting changes in flux through the pathway, particularly repression of the oxidative phase of the PPP but activation of the non-oxidative phase. This would favor the production of ribose-5-phosphate from glyceraldehyde-3-phosphate and fructose-6-phosphate (Morriss *et al.*, 2017). To compensate for the loss of recycling of nucleosides, carbon flux in *rns2-2* may therefore be diverted via the PPP toward the production of ribose-5-phosphate, which is an essential substrate in *de novo* purine synthesis (Bassham and MacIntosh, 2017; Morriss *et al.*, 2017).

If the constitutive autophagy seen in *rns2-2* mutants is related to nucleotide homeostasis, it potentially acts via known regulators. In Arabidopsis, the sucrose non-fermenting-1-related protein kinase 1 (SnRK1) complex activates autophagy during stress (Soto-Burgos and Bassham, 2017), and the mammalian homolog AMP-activated protein kinase (AMPK) is regulated by the AMP/ATP ratio (Hardie, 2011; Carroll and Dunlop, 2017), although it is not clear if this is true in plants. In addition, the Arabidopsis target of rapamycin (TOR) protein kinase complex is a negative regulator of autophagy (Liu and Bassham, 2010; Pu *et al.*, 2017), preventing activation of the pathway under conditions favoring growth. While knowledge of upstream factors controlling TOR activity in plants is limited, mammalian TOR is involved in sensing purine nucleotide levels, amino acids, and growth factors to coordinate downstream processes such as nucleic acid synthesis, ribogenesis, and growth (Iadevaia *et al.*, 2014; Emmanuel *et al.*, 2017; Hoxhaj *et al.*, 2017). In addition, mTORC1 activation promotes the *de novo* synthesis of both pyrimidine and purine nucleotides due to their heavy demand during ribogenesis (Ben-Sahra *et al.*, 2013, 2016; Robitaille *et al.*, 2013; Valvezan *et al.*, 2017). Here, we assess the potential mechanism of activation of autophagy in *rns2-2* mutants. We show that the activation of autophagy is probably due to reduced purine levels, leading to a reduction in TOR activity and in turn to autophagy activation, possibly in an attempt to compensate for reduced nucleotide levels. This work provides insight both into the function of vacuolar RNA degradation in nucleotide homeostasis and into the regulation of autophagy by nucleotide concentrations via TOR.

Materials and methods

Plant materials and growth conditions

Arabidopsis thaliana genotypes used are Col-0, green fluorescent protein (GFP)–ATG8e (Xiong *et al.*, 2007), *rns2-2* GFP–ATG8e (Floyd *et al.*, 2015), and *raptor1b* (SALK_078159) (Anderson *et al.*, 2005). Seeds were sterilized and plants grown as described previously (Pu *et al.*, 2017). In all experiments, plants were grown on solid half-strength Murashige and Skoog (1/2 MS) medium, pH 5.7 [2.22 g l^{-1} MS vitamin and salt mixture (Caisson Laboratories, MSP09), 1.5% (w/v) Phytoblend agar (Caisson Laboratories, PTP01), 20% (w/v) sucrose, and 0.05% (w/v) MES] for 7 d under long-day conditions (16 h of light) at 22 °C.

Chemical treatments

All chemicals were purchased from Sigma-Aldrich USA, unless otherwise indicated. For purine (inosine and hypoxanthine) or pyrimidine (cytidine, thymidine, and uridine) nucleoside supplementation, seedlings were grown on solid 1/2 MS medium for 7 d and transferred to liquid 1/2 MS medium supplemented to a final concentration of 10 μM, unless otherwise indicated, for 3 h.

For depletion of purines or pyrimidines, 7-day-old seedlings were transferred to liquid 1/2 MS medium supplemented with increasing concentrations of the following inhibitors; purine synthesis inhibitors:

methotrexate (MTX) or lometrexol (LTX) at 0, 2, or 5 μM final concentrations; purine salvage inhibitors: 2,6-diaminopurine (2,6-DAP) or 6-mercaptopurine (6-MP) at 0, 100, or 300 μM final concentrations; or pyrimidine synthesis inhibitors: 5-fluorouracil (5-FU) and 6-azauridine (6-AZA) at 0, 1, 5, or 10 μM final concentrations. To restore purine nucleotides after depletion, 7-day-old seedlings were transferred to liquid 1/2 MS medium supplemented to a final concentration of 5 μM LTX or MTX, or 300 μM 2,6-DAP or 6-MP, and inosine was added to 10 μM for the last 1.5 h.

To inhibit SnRK1, 7-day-old seedlings were transferred to liquid 1/2 MS medium supplemented with trehalose-6-phosphate (T6P) to a final concentration of 0.1 mM (Santa Cruz, SC216004) for 3 h (Zhang *et al.*, 2009). To activate TOR, 7-day-old seedlings were transferred to 1/2 MS liquid medium supplemented to a final concentration of 20 nM 1-naphthaleneacetic acid (NAA) or DMSO as solvent control for 6 h (Pu *et al.*, 2017). Inhibition of TOR using AZD8055 (AZD) (LC Laboratories, A-2345) was done as in Pu *et al.* (2017), with minor modifications. Briefly, seedlings were incubated with 1 μM AZD in liquid 1/2 MS medium for 3 h and the medium was supplemented with 10 μM inosine for the last 1.5 h.

Immunoblotting

Proteins were extracted from 7-day-old Arabidopsis seedlings supplemented or not with 10 μM inosine or 1 μM AZD for S6 kinase (S6K) phosphorylation assays or with purine (5 μM LTX or MTX or 300 μM 2,6-DAP or 6-MP) or pyrimidine (10 μM 5FU or 6-AZA) synthesis/salvage inhibitors for GFP cleavage assays. For ATG8 accumulation assays, seedlings were supplemented with 1 μM concanamycin A (ConcA), with or without purine or pyrimidine nucleosides (10 μM), NAA (20 nM), T6P (0.1 mM), AZD (1 μM), or purine/pyrimidine synthesis/salvage inhibitors for 12 h. Seedlings were ground in sample buffer [20% (w/v) SDS, 0.075 M Tris–HCl, pH 6.8, 25% (v/v) glycerol, 0.5% (v/v) 2-mercaptoethanol, and 0.5% (w/v) bromophenol blue]. The homogenate was centrifuged at 16 000 *g* in a benchtop microcentrifuge (Beckman Coulter Life Sciences) for 10 min at 4 °C to remove cell debris. The supernatant was heated at 95 °C for 5 min and vortexed before loading. Proteins were separated by 15% or 10% (w/v) acrylamide SDS–PAGE for ATG8 accumulation and GFP cleavage assays or S6 kinase (S6K) phosphorylation assays, respectively. Proteins were detected using a 1:1000 dilution in 5% (w/v) non-fat milk of anti-GFP (Roche Diagnostics, 1184460001) monoclonal primary antibodies or anti-ATG8a (AS14 2769, Agrisera), S6K1/2 (Agrisera, AS12 1855), or S6K1-2-phosphorylated (P-S6K) (Agrisera, AS13 2664) polyclonal primary antibodies. Blots were then probed using a 1:10 000 dilution of horseradish peroxidase (HRP)-conjugated goat anti-mouse secondary antibody (Sigma-Aldrich, AP308P) for GFP or HRP-conjugated goat anti-rabbit secondary antibody (Bio-Rad, 1706515) for P-S6K, S6K, or ATG8. Blots were scanned and bands quantified using ImageJ software (Schneider *et al.*, 2012). For GFP cleavage, the ratio of free GFP to GFP–ATG8e band intensities was used as a measure of the extent of autophagy activity, while the ratio of phosphorylated S6K to non-phosphorylated S6K indicates TOR kinase activity. For ATG8 accumulation, the band intensities were first normalized to the Ponceau S-stained Rubisco band as loading control, and all treatments were compared with wild-type untreated control set to 1 unit.

Microscopy and autophagosome quantification

Arabidopsis wild-type and *raptor1b* seedlings were stained with monodansylcadaverine (MDC) as described previously (Contento *et al.*, 2005). MDC-stained or GFP-labeled structures within the root elongation zone were counted using a Zeiss AxioImager microscope, with a ×40 objective and a DAPI-specific filter for MDC or a fluorescein isothiocyanate (FITC) filter for GFP. Data from at least nine frames constituted a sample and were used to determine the average number of autophagosomes per sample from three biological replicates unless otherwise indicated. Sample images within the root elongation zone were taken using a Leica SP5 confocal laser scanning microscope with a ×63 oil immersion objective. The excitation and emission wavelengths for GFP were 488 nm and 507 nm, respectively. All the microscopy was performed at the Roy J. Carver High Resolution Microcopy Facility at Iowa State University.

Statistical analysis

Two-tailed Student's *t*-tests were computed for pairwise comparison of means of data sets, with the statistical significance level set to 0.05. For all figures, error bars are the mean ±SEM.

Results

Purine but not pyrimidine nucleosides suppress autophagy in rns2-2 *seedlings*

Arabidopsis plants lacking RNS2 have constitutive autophagy (Hillwig *et al.*, 2011; Floyd *et al.*, 2015), but the reason for this phenotype is unknown. We hypothesized that due to impaired vacuolar rRNA turnover in *rns2* mutants, nucleoside recycling is reduced, leading to a decrease in cytosolic nucleoside and nucleotide concentrations. Autophagy would then be activated because of these reduced concentrations, potentially as an attempt to compensate by recycling nucleosides and nucleotides from other locations. To test this hypothesis, we supplemented the growth medium of *rns2-2* and wild-type seedlings, each expressing GFP–ATG8e as an autophagosome marker, with purine or pyrimidine nucleosides to assess the effect on autophagy.

First, 7-day-old GFP–ATG8e or *rns2-2* GFP–ATG8e seedlings were incubated in liquid 1/2 MS medium supplemented with increasing concentrations of inosine, a precursor for all purines (Fig. 1A), for 3 h. At 10 μM, inosine reduced the number of GFP-labeled autophagosomes in *rns2-2* GFP–ATG8e to wild-type basal autophagy levels (Fig. 1B, C). Inosine reduced the extent of autophagy in *rns2-2* GFP–ATG8e seedlings in a dose-dependent manner, while the basal autophagy seen in GFP–ATG8e seedlings was not affected (Fig. 1C). In all subsequent experiments, inosine was used at a concentration of 10 μM. Then, seedlings were treated as above, but with the medium supplemented with purine (inosine and hypoxanthine) or pyrimidine (thymidine, cytidine, and uridine) nucleosides, at the concentrations described in Meyer and Wagner (1985) and Chen *et al.* (2006) as appropriate physiological levels. While the purines suppressed the constitutive autophagy of *rns2-2*, the pyrimidines failed to rescue this phenotype (Fig. 1D), suggesting that activation of autophagy might specifically be responsive to purine nucleoside concentrations but not to pyrimidines.

While an increase in the number of GFP–ATG8e-labeled autophagosomes indicates a change in autophagy, it could potentially be due to either increased formation or decreased degradation of autophagosomes. Two different biochemical assays have been shown in Arabidopsis to measure flux through the entire autophagy pathway, leading to vacuolar degradation, the cleavage of a GFP–ATG8 fusion protein in the vacuole and the accumulation of endogenous ATG8 in the presence of the vacuolar ATPase inhibitor ConcA (Chung *et al.*, 2010; Klionsky *et al.*, 2016; Shull *et al.*, 2019) to block degradation. Here we use each of these assays, depending on the genetic background of the plants.

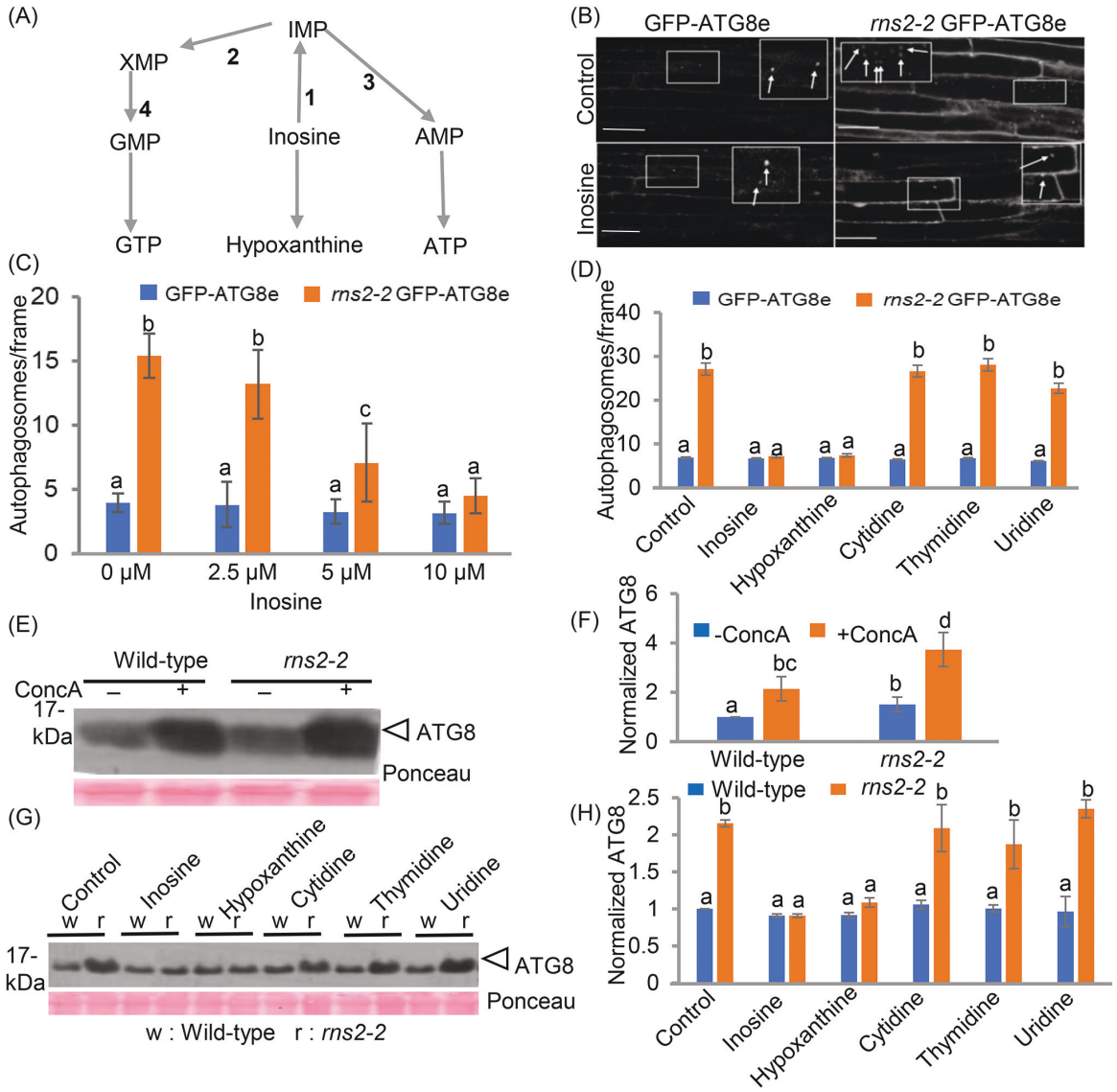

Fig. 1. Purines but not pyrimidines suppress autophagy in *rns2-2* seedlings. (A) Salvage pathway for the conversion of inosine to purine nucleotides. Enzymes: 1, inosine–guanosine kinase; 2, IMP dehydrogenase; 3, adenylosuccinate synthase; 4, GMP synthase. (B) Representative confocal images of *rns2-2* GFP–ATG8e and GFP–ATG8e seedlings after a 3 h treatment with 10 μM inosine or control without inosine. Scale bar=25 μm; white arrows indicate autophagosomes. (C) *rns2-2* GFP–ATG8e and GFP–ATG8e seedlings were treated with increasing concentrations of inosine, and GFP–ATG8e-labeled autophagosomes were quantified using epifluorescence microscopy with a GFP filter at ×40 magnification. (D) *rns2-2* GFP–ATG8e and GFP–ATG8e seedlings were treated with 10 μM final concentration of purine nucleosides (inosine and hypoxanthine) or pyrimidine nucleosides (cytidine, thymidine, or uridine) in liquid 1/2 MS medium for 3 h. GFP–ATG8e-labeled autophagosomes were quantified as in (C). Data presented in (C) and (D) are the mean ±SE for three biological replicates, n=9 frames per replicate. Statistical significance (wild type versus *rns2-2*) was determined using Student's two-tailed t-test, $P<0.05$. Different letters denote statistically significant differences between means. (E and G) *rns2-2* and wild-type seedlings were treated (E) with or without 1 μM final concentration of concanamycin A (ConcA) or (G) with nucleosides as in (D) but supplemented with 1 μM final concentration of ConcA for 12 h, and total protein was separated by SDS–PAGE followed by immunoblotting with anti-ATG8 antibodies. Shown is a representative image from three independent biological replicates. (F and H) Quantification of ATG8 band intensity, normalized to the Ponceau S-stained band corresponding to Rubisco large subunit, with the value of the wild-type control set to 1. Data are the mean ±SE for three biological replicates. Statistical significance [ConcA versus untreated control (F) or wild type versus *rns2-2* (H)] was determined using Student's two-tailed t-test, $P<0.05$. Different letters denote statistically significant differences between means. (This figure is available in color at *JXB* online.)

To confirm the suppression of the constitutive autophagy of *rns2-2* upon purine treatment, we measured accumulation of ATG8 (Yoshimoto *et al.*, 2004; Pérez-Pérez *et al.*, 2010). ATG8 localizes to both inner and outer autophagosome membranes (Kirisako *et al.*, 1999; Slobodkin and Elazar, 2013) and its expression increases upon induction of autophagy (Kirisako *et al.*, 1999; Thompson *et al.*, 2005; Xiong *et al.*, 2007; Liu *et al.*, 2009). ATG8 is delivered to the vacuole with autophagosomes and degraded, and this degradation is blocked by ConcA (Dröse *et al.*, 1993; Huss *et al.*, 2002; Dettmer *et al.*, 2006). The level of ATG8 in the presence or absence of ConcA can therefore be used as a measure of autophagic flux (Shull *et al.*, 2019).

First, wild-type or *rns2-2* seedlings were supplemented or not with ConcA (1 μM) for 12 h, after which total protein was extracted and analyzed by immunoblot using anti-ATG8 antibody to assess ATG8 accumulation. The amount

of ATG8 was higher in *rns2-2* seedlings than in the wild type, and ATG8 accumulated further in the presence of ConcA, indicating that the increase was due to enhanced autophagic flux and not decreased ATG8 degradation (Fig. 1E, F). Seedlings were then treated as in Fig. 1D but supplemented with ConcA (1 μM) and nucleosides for 12 h. The extent of ATG8 accumulation in *rns2-2* was reduced by purine but not pyrimidine nucleosides (Fig. 1G, H), in support of the hypothesis that activation of autophagy in *rns2-2* is responsive to purine but not pyrimidine nucleoside concentrations.

Autophagy is activated by depletion of purine but not pyrimidine nucleotides

The above results suggest that purines but not pyrimidines can suppress autophagy in *rns2-2* GFP–ATG8e plants. Under normal conditions, both nucleotide synthesis and nucleotide salvage contribute to maintaining homeostasis (Moffatt and Ashihara, 2002; Zrenner *et al.*, 2006; Girke *et al.*, 2014). To confirm that nucleotide depletion can activate autophagy, we treated wild-type seedlings expressing GFP–ATG8e with inhibitors of purine synthesis enzymes, purine salvage enzymes (Fig. 2A), or pyrimidine synthesis enzymes, to deplete purines or pyrimidines from the seedlings. Seedlings were transferred to liquid 1/2 MS medium supplemented with increasing concentrations of *de novo* purine synthesis inhibitors (0, 2, or 5 μM), purine salvage inhibitors (0, 100, or 300 μM), or pyrimidine synthesis inhibitors (0, 2, 5, or 10 μM) for 6 h.

Compared with the DMSO control, inhibition of the *de novo* purine synthesis enzymes dihydrofolate reductase (DHFR) with MTX (Kemper *et al.*, 1992; Loizeau *et al.*, 2008) or glycine amide ribonucleotide transformylase (GART) with LTX (Christopherson *et al.*, 2002) resulted in strong activation of autophagy in a dose-dependent manner (Fig. 2B). Similarly, inhibition of the purine salvage enzymes hypoxanthine-guanine phosphoribosyltransferase (HGPT1) with 6-MP or of adenine phosphoribosyltransferase (APT) with 2,6-DAP (Moffatt and Somerville, 1988) activated autophagy (Fig. 2C).

In contrast, inhibitors that targeted pyrimidine synthesis enzymes [5FU, which inhibits thymidylate synthase (Córdoba-Cañero *et al.*, 2010), or 6-AZA, which inhibits orotidylic acid pyrophosphorylase (Schaeffer and Sorokin, 1966; Chung and Rédei, 1974)] did not have a significant effect on autophagy under the tested conditions (Fig. 2D). These results further indicate that activation of autophagy is specifically sensitive to purines under these conditions.

To confirm that the observed activation of autophagy was caused by depletion of nucleotides, and not by other non-related inhibitor effects, we supplemented inhibitor-treated seedlings with inosine to restore purine nucleoside and hence nucleotide levels (Moffatt and Ashihara, 2002). Seedlings were transferred to liquid 1/2 MS medium supplemented with the indicated inhibitors for 6 h and inosine was added to the medium for the last 1.5 h. The number of GFP-labeled autophagosomes was significantly reduced when inosine was added to nucleotide-depleted seedlings, compared with the inhibitor treatment without inosine (Fig. 2E). These results suggest that depletion of purine nucleotides leads to activation of autophagy in Arabidopsis.

To confirm the activation of autophagy upon inhibition of purine synthesis, we used GFP–ATG8e processing (Shin *et al.*, 2014; Klionsky *et al.*, 2016) to detect autophagic flux. Once GFP–ATG8e is delivered to the vacuole by autophagy, it is degraded, resulting in free GFP (Shin *et al.*, 2014). The degree of processing thus corresponds to the extent of activation of autophagy. Seven-day-old GFP–ATG8e seedlings were incubated with 10 μM LTX, MTX, 5-FU, or 6-AZA, or 300 μM 2,6-DAP or 6-MP, with or without 10 μM inosine for 6 h. Total protein was then extracted and analyzed by immunoblot using anti-GFP antibody. Compared with the control (DMSO) treatment, purine synthesis/salvage inhibitor-treated seedlings accumulated more free GFP (Fig. 2F, G) but pyrimidine inhibitor-treated samples did not. Furthermore, inosine supplementation reduced the extent of free GFP accumulation in inhibitor-treated samples, compared with the inhibitor treatment without inosine (Fig. 2F, G), confirming that autophagy is activated upon inhibition of purine synthesis or salvage.

Autophagy activation in rns2-2 *involves TOR kinase*

We next assessed the mechanism by which autophagy is regulated by nucleotide concentrations. Two major upstream kinases regulating the activity of the autophagy pathway have been identified in plants. SnRK1, a plant ortholog of animal AMPK and yeast Snf1 (Wang *et al.*, 2001; Lee *et al.*, 2010; Hardie, 2011; Carroll and Dunlop, 2017), functions as an energy sensor that activates autophagy under low energy or nutrient conditions (Chen *et al.*, 2017; Soto-Burgos and Bassham, 2017). In contrast, TOR represses autophagy under normal, nutrient-rich growth conditions (Liu and Bassham, 2010). During nutrient starvation, salt stress, and osmotic stress, autophagy is induced in wild-type plants, while plants overexpressing TOR fail to activate autophagy under those conditions (Pu *et al.*, 2017). Therefore, we tested the possible involvement of SnRK1 and TOR in the activation of autophagy in *rns2-2*.

To determine whether SnRK1 activity is required for the constitutive autophagy seen in *rns2-2*, SnRK1 was inhibited using T6P (Zhang *et al.*, 2009). In Arabidopsis, treatment with T6P blocks autophagy activation by most abiotic stresses (Soto-Burgos and Bassham, 2017). Seven-day-old GFP–ATG8e- and *rns2-2* GFP–ATG8e-expressing seedlings were transferred to 1/2 MS liquid medium supplemented or not with 0.1 mM T6P for 3 h. GFP-labeled autophagosomes were visualized by confocal microscopy (Fig. 3A) and quantified by epifluorescence microscopy (Fig. 3B). As expected, in control conditions, GFP–ATG8e seedlings had a low basal level of autophagy, while in *rns2-2* GFP-ATG8e seedlings, autophagy was active (Fig. 3A, B). Inhibition of SnRK1 by T6P had no effect on autophagy activity in GFP–ATG8e control seedlings or in the *rns2-2* GFP–ATG8e mutant when compared with the untreated control (Fig. 3A, B). These results suggest that the constitutive autophagy activity observed in the *rns2-2* mutant is not due to aberrant activation of the SnRK1 complex.

Next, we tested whether decreased TOR kinase activity is responsible for the increased autophagy in *rns2-2*. TOR

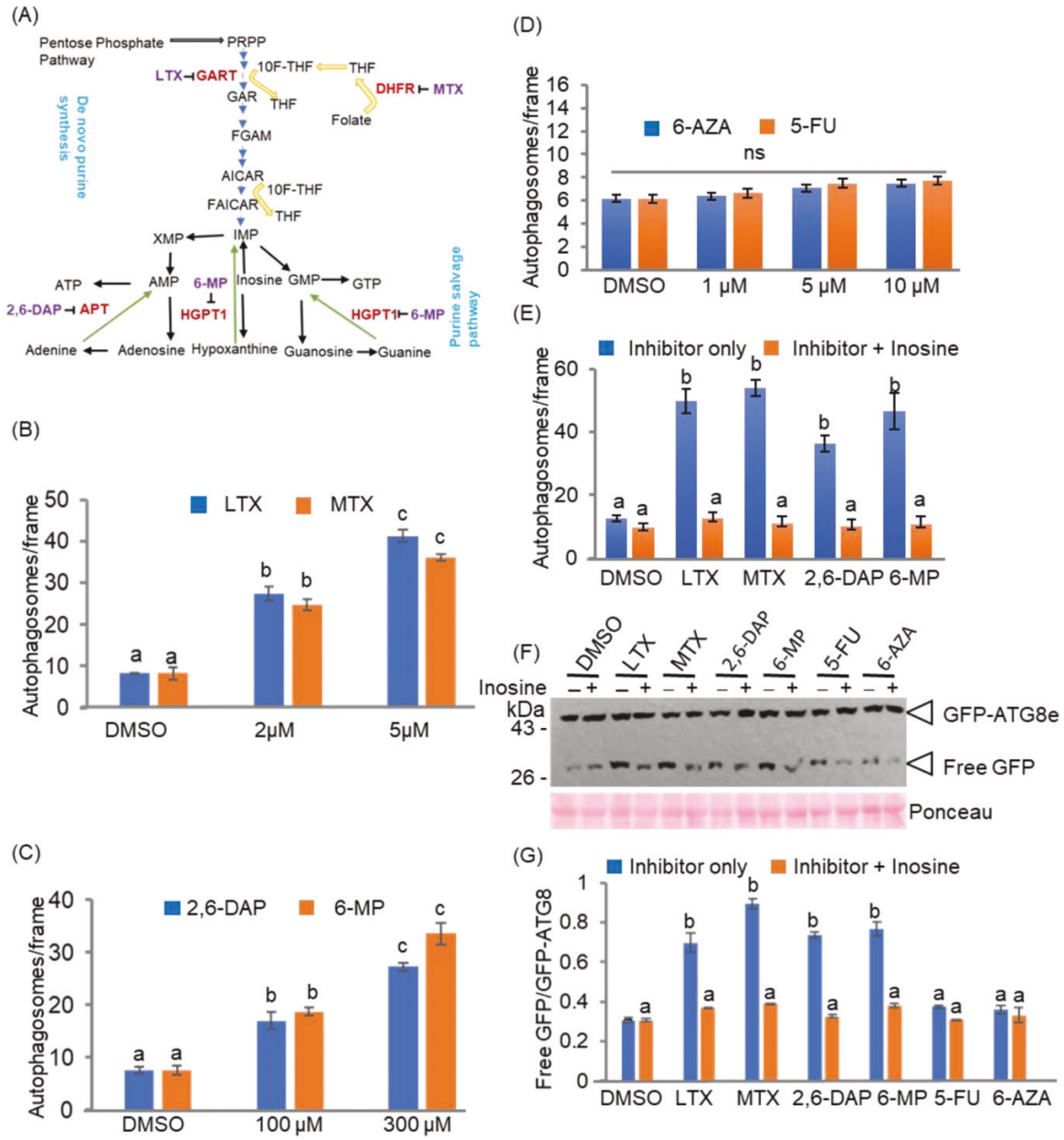

Fig. 2. Autophagy is activated by depletion of purine but not pyrimidine nucleotides. (A) Schematic diagram of the *de novo* and salvage purine synthesis pathways with key enzymes as follows: dihydrofolate reductase (DHFR), glycine amide ribonucleotide transformylase (GART), adenine phosphoribosyltransferase (APT), and hypoxanthine-guanine phosphoribosyltransferase (HGPT1). Inhibitors of specific enzymes are indicated: lometrexol (LTX), methotrexate (MTX), 2,6-diaminopurine (2,6-DAP), and 6-mercaptopurine (6-MP). Metabolites: 5-phosphoribosyl-1-pyrophosphate (PRPP), glycineamide ribonucleotide (GAR), formyl glycine amidine ribonucleotide (FGAM), 5-aminoimidazole-4-carboxyamide ribonucleotide (AICAR), 5-formamidoimidazole-4-carboxyamide ribonucleotide (FAICAR), tetrahydrofolate (THF), 10-formyl-tetrahydrofolate (10F-THF), IMP, AMP, GMP, XMP, ATP, and GTP. (B–D) Seven-day-old GFP–ATG8e seedlings were treated for 6 h in liquid 1/2 MS medium supplemented with the indicated concentrations of (B) purine synthesis inhibitors LTX or MTX, (C) purine salvage enzyme inhibitors 2,6-DAP or 6-MP, or (D) pyrimidine synthesis enzyme inhibitors 5-fluorouracil (5-FU) or 6-azauridine (6-AZA). GFP–ATG8e-labeled autophagosomes were quantified using a Zeiss AxioImager with a GFP filter at ×40 magnification. Data presented are the mean ±SE (n=9) of four biological replicates. Statistical significance (all treatments versus the DMSO control) was determined using Student's t-test, P<0.05. Different letters denote statistically significant differences between means. (E) Seven-day old GFP–ATG8e seedlings were treated for 6 h in liquid 1/2 MS medium supplemented with DMSO as a control, LTX or MTX (5 μM), or 2,6-DAP or 6-MP (300 μM). After 4.5 h of inhibitor treatment, inosine was added to the samples for 1.5 h and autophagosomes were counted. Data presented are the mean ±SE (n=9) of three biological replicates. Statistical significance (inhibitor only versus inhibitor plus inosine treatments) was determined using Student's t-test, P<0.05. Different letters denote statistically significant differences between means. (F) Seven-day-old GFP–ATG8e seedlings were incubated for 6 h in liquid 1/2 MS medium supplemented with DMSO as a control, LTX or MTX (5 μM), 2,6-DAP or 6-MP (300 μM), or 5-FU or 6-AZA (10 μM), each with or without 10 μM inosine, and total protein was separated by SDS–PAGE followed by immunoblotting with anti-GFP antibodies. Data shown are a representative image of three different experiments. (G) Quantification of the ratio between free GFP and GFP–ATG8e. Data are the mean ±SE for three biological replicates. Statistical significance (inhibitor only versus inhibitor plus inosine treatments) was determined using Student's two-tailed t-test, P<0.05. Different letters denote statistically significant differences between means. (This figure is available in color at *JXB* online.)

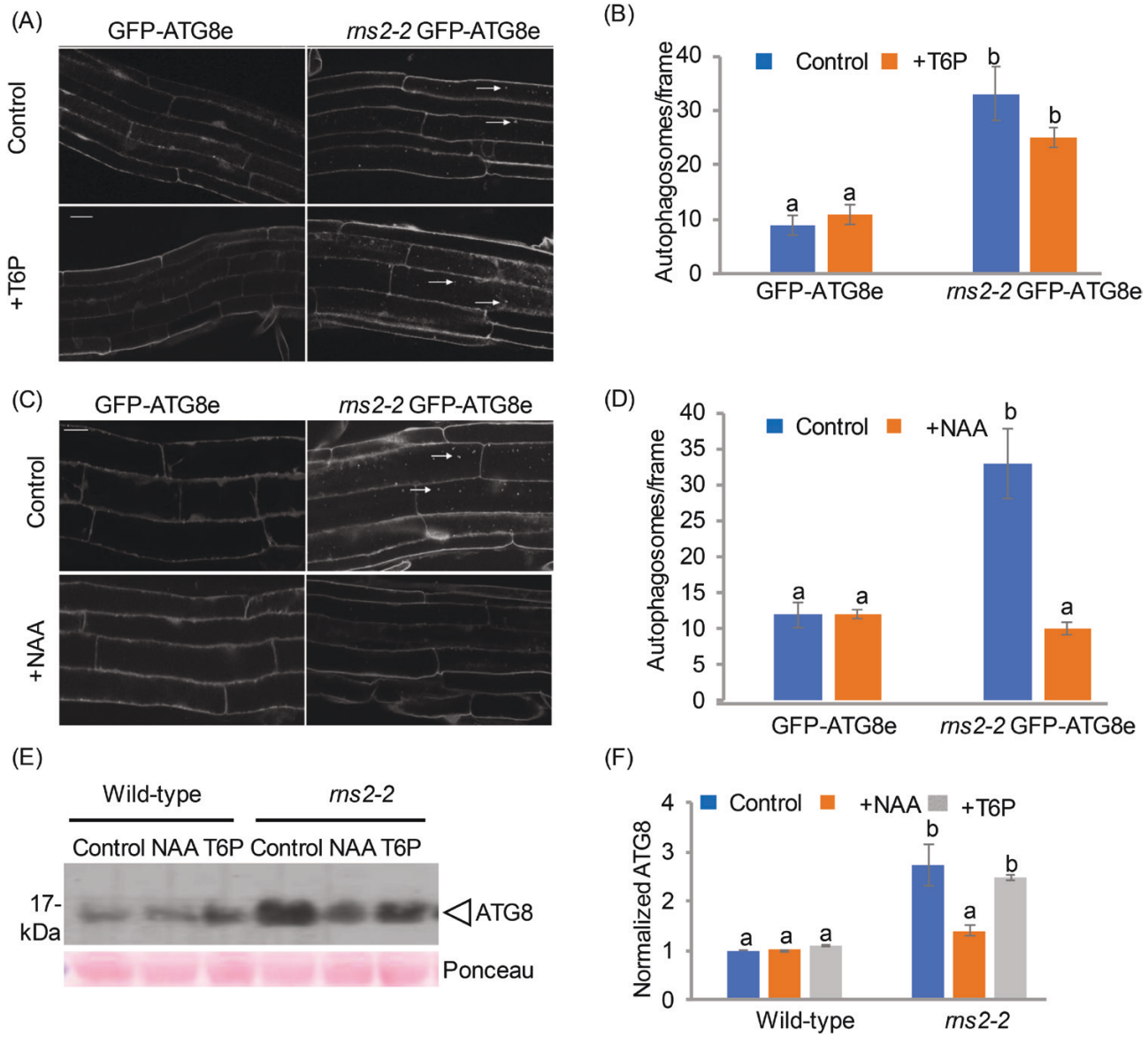

Fig. 3. Autophagy in *rns2-2* is dependent on repression of TOR kinase. (A, C) Seven-day-old GFP–ATG8e and *rns2-2* GFP–ATG8e seedlings were transferred to 1/2 MS liquid medium supplemented to a final concentration of (A) 0.1 mM T6P or DMSO for 3 h or (C) 20 mM NAA or DMSO for 6 h. Representative confocal images show autophagosomes (white arrows) in roots. Scale bar=25 μm. (B, D) Quantification of GFP–ATG8e-labeled autophagosomes treated as in (A) or (C) using epifluorescence microscopy. Data presented are the mean ±SE for three biological replicates (n=9 frames per replicate). Statistical significance (all treatments versus DMSO control) was determined using Student's t-test, $P<0.05$. Different letters denote statistically significant differences between means. (E) Seven-day-old wild-type or *rns2-2* seedlings were treated as in (A) or (C) but supplemented with 1 μM final concentration of ConcA for 12 h, and total protein was separated by SDS–PAGE followed by immunoblotting with anti-ATG8 antibodies. Data shown are a representative image of three different experiments. (F) Quantification of the ratio between ATG8 and Ponceau S-stained Rubisco large subunit band, with the wild-type control set to 1. Data are the mean ±SE for four biological replicates. Statistical significance (all treatments versus DMSO control) was determined using Student's two-tailed t-test, $P<0.05$. Different letters denote statistically significant differences between means. (This figure is available in color at *JXB* online.)

kinase can be activated by exogenous auxin (Schepetilnikov *et al.*, 2013, 2017), which in turn represses autophagy during nutrient starvation, salt stress, and osmotic stress (Pu *et al.*, 2017). Seven-day-old GFP–ATG8e- and *rns2-2* GFP–ATG8e-expressing seedlings were transferred to 1/2 MS liquid medium supplemented with 20 nM of the auxin NAA for 6 h, or with DMSO as solvent control. After treatment, seedlings were visualized by confocal microscopy (Fig. 3C) or epifluorescence microscopy for quantification (Fig. 3D). In control conditions, GFP–ATG8e seedlings have a low basal level of autophagy while in *rns2-2* GFP–ATG8e seedlings, autophagy is active (Fig. 3C, D). Activation of TOR kinase by NAA had no effect on the autophagy activity in GFP–ATG8e seedlings when compared with the solvent control (Fig. 3C, D). In *rns2-2* GFP–ATG8e seedlings, the constitutive autophagy seen under control conditions was blocked upon activation of the TOR kinase by NAA treatment (Fig. 3C, D).

To confirm these results, wild-type and *rns2-2* seedlings were treated with T6P or NAA, together with ConcA, for 12 h, after

which total protein was extracted and immunoblotted using anti-ATG8 antibody. The extent of ATG8 accumulation was not affected by T6P in either *rns2-2* or wild-type seedlings (Fig. 3E, F). In contrast, ATG8 accumulation in *rns2-2* seedlings was reduced by NAA treatment. Together, these results suggest that the increased autophagy in *rns2-2* may be due to decreased activity of TOR, which can be overcome by activation with auxin.

Purine nucleosides are upstream inputs into the TOR autophagy pathway

TOR activity is determined by cellular conditions, including the availability of nutrients, for example amino acids and glucose, and hormone signaling, primarily auxin (Liao *et al.*, 2008; Schepetilnikov *et al.*, 2013, 2017; Xiong *et al.*, 2013). TOR is activated when nutrients are abundant but repressed upon nutrient deficiency, leading to activation of autophagy (Arsham and Neufeld, 2006; Liao *et al.*, 2008). Phosphoproteomics and yeast two-hybrid assays revealed possible interactions between Arabidopsis TOR and enzymes involved in nucleotide synthesis (Arabidopsis Interactome Mapping Consortium, 2011; Van Leene *et al.*, 2019). In mammalian cells, TOR is involved in regulation of nucleotide synthesis (Robitaille *et al.*, 2013) and in sensing purine nucleotide levels to ensure that ribosomes are made only when there are abundant nucleotides (Emmanuel *et al.*, 2017; Hoxhaj *et al.*, 2017).

To assess the relationship between activation of autophagy by TOR and by nucleotide concentrations, 7-day-old wild-type or *raptor1b* (a knockout mutant of the TOR subunit RAPTOR1B) (Anderson *et al.*, 2005; Deprost *et al.*, 2005) mutant seedlings were incubated in liquid 1/2 MS medium with or without a 10 μM final concentration of inosine for 3 h. As lines containing the GFP–ATG8e marker are not available in the *raptor1b* genetic background, we stained the seedlings with the fluorescent dye MDC (Biederbick *et al.*, 1995), which stains primarily autophagic structures in Arabidopsis roots in our experimental conditions (Floyd *et al.*, 2015). For immunoblot analysis, seedlings were incubated in liquid 1/2 MS medium supplemented with ConcA, and with or without a 10 μM final concentration of inosine for 12 h. Proteins were extracted and immunoblotted using anti-ATG8 antibody. As shown previously, *raptor1b* seedlings have constitutive autophagy due to reduced TOR activity (Pu *et al.*, 2017). Inosine was unable to suppress the constitutive autophagy in *raptor1b* mutant seedlings (Fig. 4A) and ATG8 accumulated in both inosine-treated and untreated *raptor1b* mutant seedlings (Fig. 4B, C), consistent with the hypothesis that inosine acts upstream of TOR in the autophagy pathway.

To confirm these data, we made use of AZD8055 (AZD) (Chresta *et al.*, 2010), an ATP-competitive inhibitor of TOR kinase (Li *et al.*, 2015) that activates autophagy in Arabidopsis (Pu *et al.*, 2017). Seven-day old GFP–ATG8e and *rns2-2* GFP–ATG8e seedlings were supplemented to a final concentration of 1 μM AZD, 10 μM inosine, or a combination of AZD and inosine (inosine added for the last 1.5 h), and autophagy was quantified after 3 h. For immunoblot analysis, wild-type and *rns2-2* seedlings were treated as above, but the medium was supplemented with ConcA for 12 h and blots were probed using anti-ATG8 antibody. Upon treatment with AZD, autophagy was active in both GFP–ATG8e and *rns2-2* GFP–ATG8e seedlings, and inosine was unable to block this autophagy (Fig. 4D). Furthermore, inosine failed to block ATG8 accumulation in the presence of AZD in both wild-type and *rns2-2* seedlings (Fig. 4E, F). Therefore, the effect of inosine on autophagy requires active TOR, and inosine has no effect when TOR activity is disrupted (in *raptor1b*; Fig. 4A–C) or when TOR is inhibited by AZD in either wild-type or *rns2-2* seedlings (Fig. 4D–F). Taken together, these results indicate that in *rns2-2*, the suppression of autophagy by inosine is dependent on TOR kinase and suggest that inosine (or, more broadly, purine nucleosides) acts as an upstream input into the TOR autophagy pathway.

We hypothesized that, as in mammals (Emmanuel *et al.*, 2017; Hoxhaj *et al.*, 2017), Arabidopsis TOR is activated in nucleotide-replete conditions and, therefore, TOR might be repressed in *rns2-2* mutants due to reduced cytoplasmic nucleotide concentrations. To test this possibility, we determined TOR activity in *rns2-2* mutant seedlings, compared with wild-type seedlings, by immunoblotting using antibodies against the known TOR substrate S6 kinase (S6K) (Turck *et al.*, 2004), which stimulates protein synthesis through phosphorylation of ribosomal S6 proteins (Dobrenel *et al.*, 2016). If TOR kinase activity is reduced in *rns2-2* mutants, we expect to see reduced phosphorylation of S6K by TOR kinase relative to the wild type under normal growth conditions. Seven-day-old *rns2-2* and wild-type seedlings were incubated in 1/2 MS liquid medium supplemented or not with AZD (1 μM), and total protein was extracted and analyzed by immunoblot using anti-S6K1/2 antibodies (Xiong and Sheen, 2012; Xiong *et al.*, 2013) and the phosphospecific anti-P-S6K1-2 antibodies (Dong *et al.*, 2019). As shown in Fig. 5A and B, the phosphorylation of S6K in the *rns2-2* mutant was reduced compared with that in wild-type seedlings. Upon treatment with AZD, the phosphorylation of S6K by TOR was substantially reduced in wild-type and completely abolished in *rns2-2* seedlings (Fig. 5A, B), verifying that the species with an apparent molecular mass of 60 kDa is P-S6K. However, when *rns2-2* seedlings were supplemented with inosine for 3 h, S6K was phosphorylated to a similar extent as in wild-type seedlings (Fig. 5C, D). Taken together, these results indicate that TOR kinase activity is repressed in *rns2-2* due to reduced nucleoside concentrations, and that restoration of nucleoside concentrations by exogenous supplementation of inosine to seedlings restores TOR activity.

Discussion

Ribosome turnover in eukaryotes is important for maintaining cellular homeostasis both in response to nutrient deficiency (Kraft *et al.*, 2008; Huang *et al.*, 2015) and under normal conditions (Kazibwe *et al.*, 2019). In yeast and animals, several pathways involved in the degradation of non-functional ribosomes and misassembled ribosome subunits have been described (Houseley and Tollervey, 2009; Lafontaine, 2010). However, the fate of mature ribosomes or their components, in particular

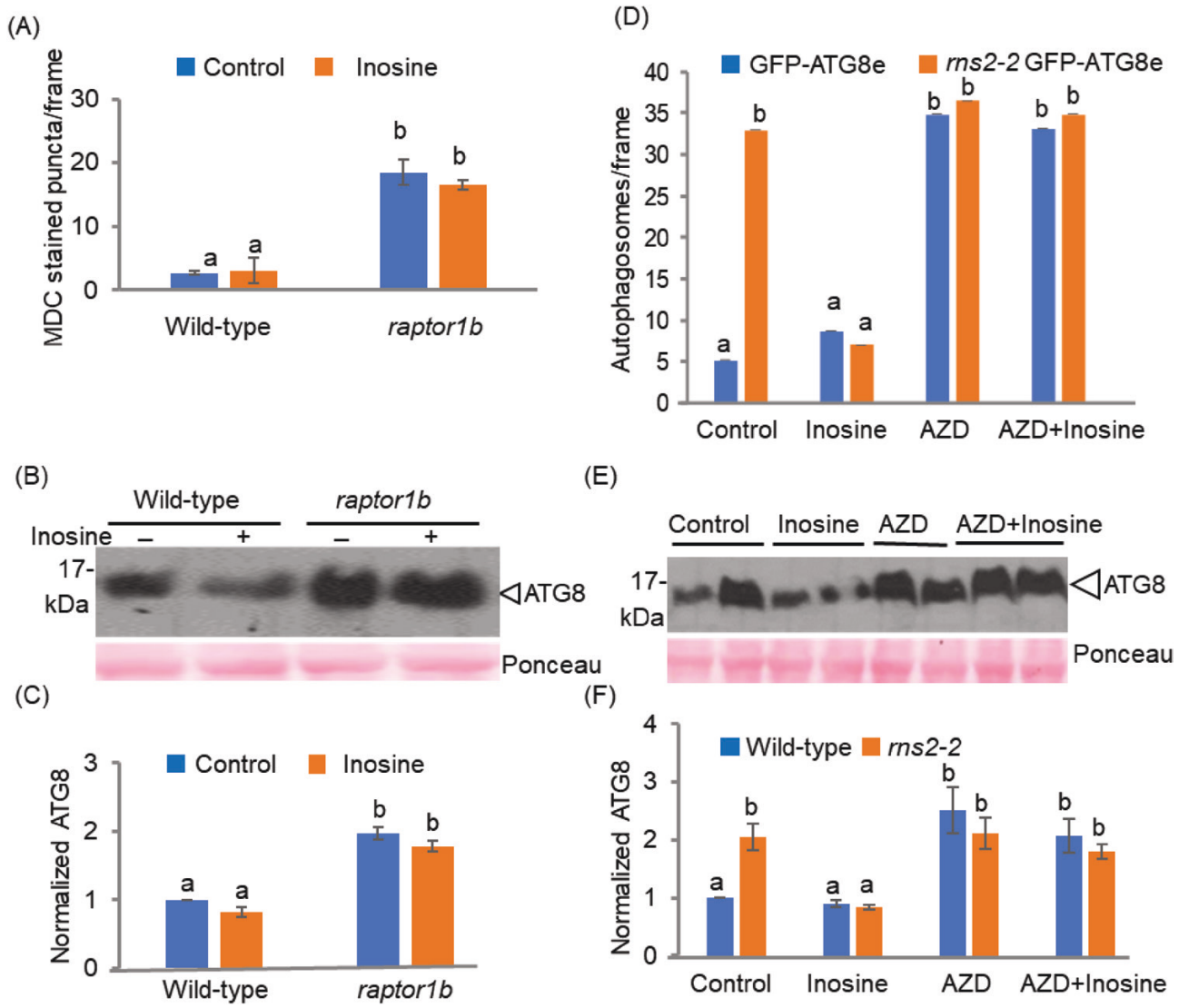

Fig. 4. Inosine acts upstream of TOR in activation of autophagy. (A) Seven-day-old wild-type or *raptor1b* mutant seedlings were transferred to liquid 1/2 MS medium with or without 10 μM inosine for 3 h. The seedlings were stained with MDC, and fluorescent puncta were quantified using epifluorescence microscopy. Data presented are the mean ±SE for three biological replicates (n=9 frames per replicate). Statistical significance (inosine versus the DMSO control) was determined using Student's t-test, P<0.05. Different letters denote statistically significant differences between means. (B) Seedlings were treated as in (A) but the medium was supplemented with 1 μM ConcA for 12 h, and total protein was separated by SDS–PAGE followed by immunoblotting with anti-ATG8 antibodies. Data shown are a representative image of four different experiments. (C) Quantification of the ratio between ATG8 and the Ponceau S-stained Rubisco large subunit band, with the wild-type control set to 1. Data are the mean ±SE for four biological replicates. Statistical significance (inosine versus the DMSO control) was determined using Student's two-tailed t-test, P<0.05. Different letters denote statistically significant differences between means. (D) Seven-day-old GFP–ATG8e or *rns2-2* GFP–ATG8e seedlings were transferred to liquid 1/2 MS medium supplemented with DMSO as a control, inosine (10 μM), AZD (1 μM) for 3 h, or AZD (1 μM) plus inosine (added after 1.5 h). GFP–ATG8e-labeled autophagosomes were quantified using epifluorescence microscopy with a GFP filter at ×40 magnification. Data presented are the mean ±SE for three biological replicates, n=9 frames per replicate. Statistical significance (*rns2*-2 versus wild type) was determined using Student's t-test, P< 0.05. Different letters denote statistically significant differences between means. (E) Seedlings were treated as in (D) but the medium was supplemented with 1 μM ConcA for 12 h, and total protein was separated by SDS–PAGE followed by immunoblotting with anti-ATG8 antibodies. Data shown are a representative image of four different experiments. (F) Quantification of the ratio between ATG8 and Ponceau S-stained Rubisco large subunit band, with the wild-type control set to 1. Data are the mean ±SE for four biological replicates. Statistical significance (*rns2*-2 versus wild type) was determined using Student's two-tailed t-test, P<0.05. Different letters denote statistically significant differences between means. (This figure is available in color at *JXB* online.)

rRNA, at the end of their useful life remains unclear. Vacuolar rRNA turnover, at least in yeast, results in nucleosides which are recycled to the cytoplasm and excreted (Huang *et al.*, 2015), while, in plants, the recycled nucleosides may be used in primary metabolism such as nucleic acid synthesis (Stasolla *et al.*, 2006). However, in the *rns2-2* mutant, rRNA turnover is impaired (Hillwig *et al.*, 2011; Floyd *et al.*, 2015), and therefore nucleosides are not recycled. This may reduce cytosolic nucleoside and nucleotide pools, potentially constituting a signal that activates autophagy (Hillwig *et al.*, 2011; Morriss *et al.*, 2017).

We propose a model for the recycling of nucleosides from vacuolar rRNA turnover and the involvement of the TOR kinase complex in sensing these nucleosides to regulate autophagy. In wild-type plants, degradation of rRNA by

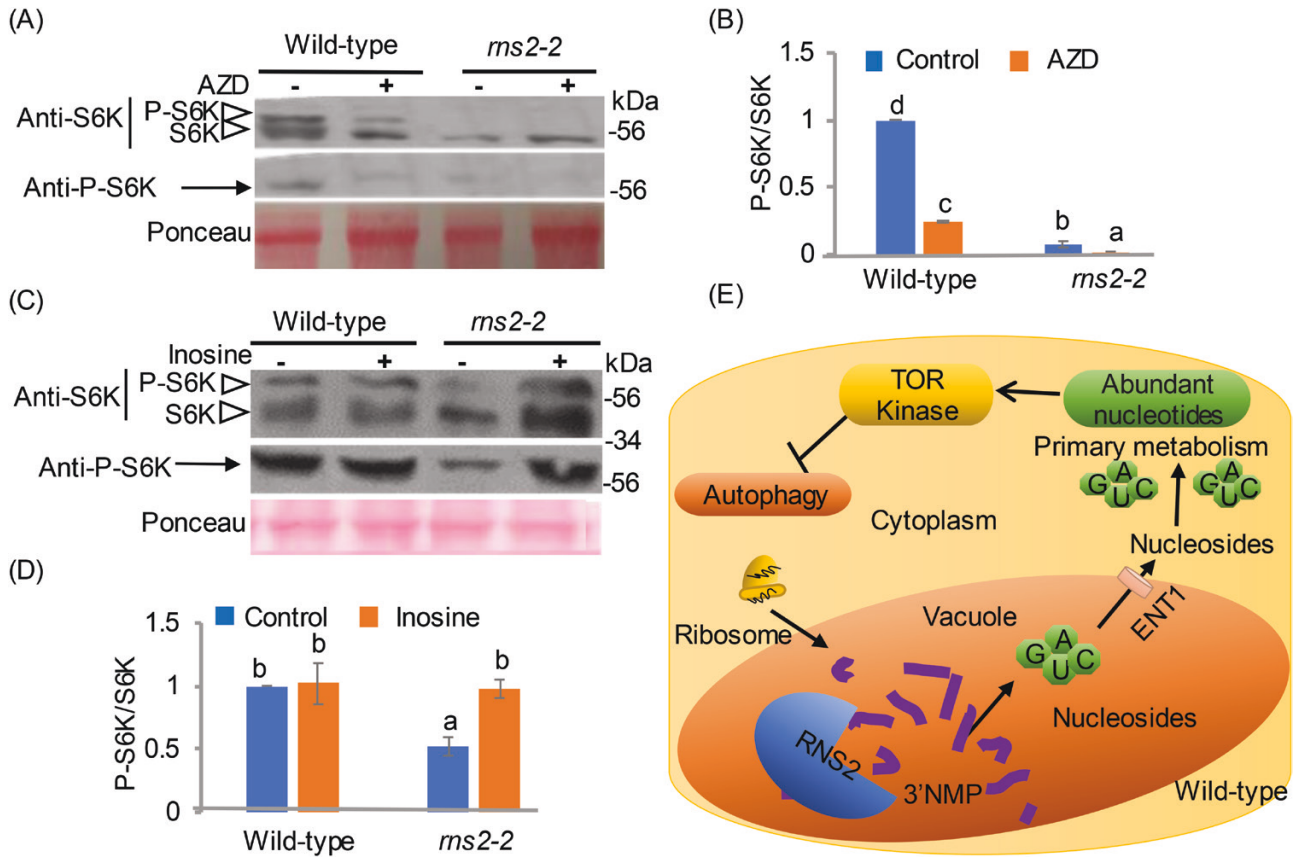

Fig. 5. TOR kinase activity is reduced in *rns2-2*. (A) Seven-day-old *rns2-2* and wild-type seedlings were incubated in 1/2 MS liquid medium supplemented or not with AZD (1 μM), and total protein was extracted and analyzed by immunoblot using anti-S6K and anti-phospho-S6K antibodies. Data shown are a representative image of three different experiments. (B) Quantification of the ratio between P-S6K and S6K. The value for P-S6K/S6K in the wild-type control was set to 1. Data are the mean ±SE for three biological replicates. Statistical significance (DMSO control versus AZD treatment) was determined using Student's two-tailed *t*-test, $P<0.05$. Different letters denote statistically significant differences between means. (C) Seven-day-old *rns2-2* and wild-type seedlings were transferred to liquid 1/2 MS medium supplemented with DMSO or inosine (10 μM) for 3 h. Total protein was then extracted and analyzed by immunoblot using anti-S6K and anti-phospho-S6K antibodies. (D) Quantification of the ratio between P-S6K and S6K. The value for P-S6K/S6K in wild-type DMSO was set to 1. Data are the mean ±SE for three biological replicates. Statistical significance (DMSO versus inosine treatments) was determined using Student's two-tailed *t*-test, $P<0.05$. Different letters denote statistically significant differences between means. (E) Proposed working model for the nucleotide-dependent activation of autophagy by TOR kinase. Ribosome degradation in vacuoles results in 3' nucleoside monophosphates (3'NMPs) which are dephosphorylated into nucleosides. The resulting nucleosides are transported to the cytoplasm by tonoplast-localized Equilibrative Nucleoside Transporter 1 (ENT1), where they are used in primary metabolism. In wild-type plants under normal growth conditions, nucleotides are abundant, and TOR is active, resulting in low basal autophagy. In *rns2-2,* the loss of rRNA turnover results in reduced nucleoside recycling and, ultimately, a low cytosolic nucleoside concentration, which represses TOR and activates autophagy. (This figure is available in color at *JXB* online.)

RNS2 recycles nucleosides that are then transported from the vacuole to the cytoplasm where they are converted to nucleotides and used in primary metabolism. Appropriate levels of nucleosides/nucleotides ensure that TOR is activated, resulting in low basal autophagy. The defect in rRNA degradation in *rns2-2* leads to decreased cytoplasmic purine nucleoside/nucleotide concentrations, reducing TOR activity, and causing autophagy induction (Fig. 5E).

The expression of RNases such as RNS2 is regulated in different environmental conditions in order to maintain cellular function. For example, during phosphate starvation and senescence, RNS2 is up-regulated, possibly to remobilize the phosphate in RNA (Taylor *et al.*, 1993; Bariola *et al.*, 1999). In contrast, under hypoxia, maize roots show reduced overall RNase activity, probably including the maize ortholog of RNS2, reducing degradation of RNA or ribosomes (Fennoy *et al.*, 1997). This potentially maintains a functional complement of ribosomes when environmental conditions reduce ribosome synthesis. As in other organisms such as yeast (Liu *et al.*, 2018), the degradation of rRNA in plants seems essential for nucleotide homeostasis.

The *de novo* purine synthesis and salvage pathways converge at IMP, and inosine can be converted to all other purine nucleotides (Figs 1A, 2A) (Moffatt and Ashihara, 2002; Zrenner *et al.*, 2006). To ascertain whether there is a relationship between autophagy and nucleoside concentration, we supplemented seedlings with exogenous nucleosides, and also depleted nucleotides using known inhibitors of nucleotide synthesis or salvage enzymes. In *rns2-2* mutant seedlings, the constitutive autophagy phenotype is blocked by restoration of nucleotide pools through exogenous supplementation of these seedlings with purine nucleosides (Fig. 1). Blocking nucleotide synthesis results in a similar increase in autophagy (Fig. 2), indicating that reduced nucleoside or nucleotide levels in the

rns2-2 mutant can be at least one of the signals that trigger the constitutive autophagy phenotype. This view is supported by the gene expression and metabolic profile data for *rns2-2* that determined that the PPP is differentially regulated in the mutant (Morriss *et al.*, 2017). In *rns2-2*, the PPP enzymes may be regulated in order to divert the carbon flux toward production of ribose-5-phosphate for *de novo* purine synthesis, possibly to compensate for the loss of recycling of nucleosides. However, which specific nucleotides and/or nucleosides are sensed, and the identity of the sensors of their concentrations in plants are unknown.

Our data show that purine but not pyrimidine nucleosides reduce autophagy in *rns2-2* seedlings, suggesting that autophagy activation in *rns2-2* is specifically sensitive to intracellular purine levels under our experimental conditions. This observation is comparable with the data from mammalian cell studies in which TOR activity is sensitive to changes in intracellular purine levels but not to pyrimidine levels (Emmanuel *et al.*, 2017; Hoxhaj *et al.*, 2017). In plants, whether a specific purine or a derived metabolite is the signal involved in sensing of nucleoside concentrations is unknown.

In Arabidopsis, regulators of autophagy include the ATG1 complex, which activates autophagy in stress conditions such as nutrient starvation (Suttangkakul *et al.*, 2011), IRE1b, which acts in response to endoplasmic reticulum stress (Liu *et al.*, 2012), the TOR complex, a negative regulator of autophagy under starvation, salt, and osmotic stress (Liu and Bassham, 2010; Pu *et al.*, 2017), and SnRK1, a positive regulator of autophagy in response to stress (Chen *et al.*, 2017; Soto-Burgos and Bassham, 2017). SnRK1 acts as an energy sensor, activating multiple signaling pathways in response to low energy levels (Baena-González *et al.*, 2007; Margalha *et al.*, 2019). Inhibition of SnRK1 by T6P in the *rns2-2* mutant did not lead to changes in autophagy activity (Fig. 3). Transcriptomic analysis of the *rns2-2* mutant indicated that these plants are not in a nutrient deficit, and that there is a significant negative correlation between genes that are differentially expressed in the mutant with targets of KIN10 (catalytic subunit of SnRK1) regulation (Morriss *et al.*, 2017), suggesting that the SnRK1 pathway might be repressed in the *rns2-2* mutant.

The TOR complex regulates nutrient-responsive processes, such as growth, translation, and autophagy (Anderson *et al.*, 2005; Deprost *et al.*, 2005; Liu and Bassham, 2010; Moreau *et al.*, 2012). RAPTOR is a substrate-binding subunit of the TOR complex (Hara *et al.*, 2002) and has two isoforms in Arabidopsis, RAPTOR1A and RAPTOR1B (Anderson *et al.*, 2005; Deprost *et al.*, 2005). A *raptor1b* mutant has constitutive autophagy, while transgenic lines that overexpress TOR have reduced autophagy in stress conditions (Pu *et al.*, 2017). While inosine blocked autophagy in *rns2-2* seedlings, it failed to block autophagy in *raptor1b* mutant seedlings (Fig. 4A–C), or in the presence of a TOR inhibitor (Fig. 4D–F), implying that inosine acts upstream of TOR kinase activity. The phytohormone auxin activates Arabidopsis TOR kinase (Schepetilnikov *et al.*, 2013, 2017) resulting in decreased autophagy (Pu *et al.*, 2017), and addition of auxin to the *rns2-2* mutant inhibited the autophagy activity (Fig. 3C–F). Consistent with these results, TOR kinase activity is suppressed in the *rns2-2* mutant, most probably leading to the constitutive autophagy phenotype (Hillwig *et al.*, 2011), and this suppression is rescued by the addition of inosine (Fig. 5).

Thus, we demonstrated that the autophagy phenotype observed in *rns2-2* mutants is mediated by a decrease in TOR activity, probably as a result of depleted purine levels (Figs 3–5). In mammals, intracellular nucleotide sensing is through the TSC–Rheb complex, which inhibits TOR activity when nucleotides are limiting (Ben-Sahra *et al.*, 2016; Emmanuel *et al.*, 2017; Hoxhaj *et al.*, 2017). Rheb is a small GTPase whose activity is inhibited by low nucleotide concentration, resulting in repression of TOR, and thus ensuring that TOR initiates ribogenesis only when nucleotides and other substrates are abundant (Hoxhaj *et al.*, 2017; Valvezan *et al.*, 2017). Because there are no direct plant homologs of the TSC–Rheb complex, the upstream regulators of TOR in plants are still speculative and remain unexplored. However, some upstream regulators of Arabidopsis TOR such as Rho-related protein 2 (ROP2) have been reported (Li *et al.*, 2017; Schepetilnikov *et al.*, 2017). ROP2 is a small GTPase which promotes activation of TOR and translation reinitiation of upstream ORF-containing mRNAs when activated by auxin. Whether ROP2 is involved in nucleotide sensing by TOR remains to be determined.

Our observation that depletion of purine nucleotides by inhibiting their synthesis resulted in increased autophagy in wild-type seedlings (Fig. 2) could also indicate a possible interaction between the autophagy machinery and the nucleotide biosynthesis pathway. In mammalian cells, blocking purine synthesis with inhibitors depletes intracellular nucleotides and causes DNA replication stress and cell death (Valvezan *et al.*, 2017), and reduced mTOR activity as measured by reduced phosphorylation of S6K1 by TOR (Hoxhaj *et al.*, 2017). TOR kinase is a component of a regulatory network that controls both downstream anabolic processes (Dobrenel *et al.*, 2016) and autophagy, depending on environmental signals and cellular conditions (Liu *et al.*, 2012; Pu *et al.*, 2017). Yeast two-hybrid assays and a combined phosphoproteomics screen and targeted protein complex analysis revealed a strong direct interaction of TOR with thymidylate synthase 1 (THY-1), an enzyme that links nucleotide and folate synthesis (Arabidopsis Interactome Mapping Consortium, 2011; Van Leene *et al.*, 2019). Here, we observed reduced activity of TOR in *rns2-2*, which was restored by supplementation with inosine. (Fig. 5). These data reinforce the view that there could be unexplored links between TOR-regulated autophagy and nucleotide biosynthesis in plant cells.

In conclusion, we show here that the constitutive autophagy observed in plants defective in RNS2 activity can be repressed by exogenous supplementation with purine nucleosides such as inosine, which activate the TOR signaling pathway. In our proposed model (Fig. 5E), repression of TOR in response to reduced cytosolic purine levels leads to activation of autophagy in *rns2-2*. In contrast, the abundant nucleotides in wild-type plants under normal growth conditions ensure active TOR and low basal autophagy. Still unknown are the factors that sense nucleoside/nucleotide levels and act upstream of or interact with TOR to mediate autophagy responses in the face of compromised nucleotide homeostasis.

Acknowledgements

We thank Margaret Carter for assistance with confocal microscopy. This work was supported by grant no. MCB-1714996 from the US National Science Foundation to GCM and DCB.

Author contributions

Conceptualization, DCB and GCM; funding acquisition, DCB and GCM; investigation, ZK and JSB; project administration, DCB and GCM; supervision, DCB; writing—original draft preparation, ZK; writing—review and editing, DCB and GCM.

Data availability

All data supporting the findings of this study are available within the paper.

References

Anderson GH, Veit B, Hanson MR. 2005. The Arabidopsis AtRaptor genes are essential for post-embryonic plant growth. BMC Biology **3**, 12.

Arabidopsis Interactome Mapping Consortium. 2011. Evidence for network evolution in an Arabidopsis interactome map. Science **333**, 601–607.

Arsham AM, Neufeld TP. 2006. Thinking globally and acting locally with TOR. Current Opinion in Cell Biology **18**, 589–597.

Baena-González E, Rolland F, Thevelein JM, Sheen J. 2007. A central integrator of transcription networks in plant stress and energy signalling. Nature **448**, 938–942.

Bariola PA, MacIntosh GC, Green PJ. 1999. Regulation of S-like ribonuclease levels in Arabidopsis. Antisense inhibition of RNS1 or RNS2 elevates anthocyanin accumulation. Plant Physiology **119**, 331–342.

Bassham DC, MacIntosh GC. 2017. Degradation of cytosolic ribosomes by autophagy-related pathways. Plant Science **262**, 169–174.

Ben-Sahra I, Howell JJ, Asara JM, Manning BD. 2013. Stimulation of de novo pyrimidine synthesis by growth signaling through mTOR and S6K1. Science **339**, 1323–1328.

Ben-Sahra I, Hoxhaj G, Ricoult SJH, Asara JM, Manning BD. 2016. mTORC1 induces purine synthesis through control of the mitochondrial tetrahydrofolate cycle. Science **351**, 728–733.

Bernard C, Traub M, Kunz HH, Hach S, Trentmann O, Möhlmann T. 2011. Equilibrative nucleoside transporter 1 (ENT1) is critical for pollen germination and vegetative growth in Arabidopsis. Journal of Experimental Botany **62**, 4627–4637.

Biederbick A, Kern HF, Elsässer HP. 1995. Monodansylcadaverine (MDC) is a specific in vivo marker for autophagic vacuoles. European Journal of Cell Biology **66**, 3–14.

Carroll B, Dunlop EA. 2017. The lysosome: a crucial hub for AMPK and mTORC1 signalling. The Biochemical Journal **474**, 1453–1466.

Chen KL, Xu MX, Li GY, Liang H, Xia ZL, Liu X, Zhang JS, Zhang AM, Wang DW. 2006. Identification of AtENT3 as the main transporter for uridine uptake in Arabidopsis roots. Cell Research **16**, 377–388.

Chen L, Su ZZ, Huang L, Xia FN, Qi H, Xie LJ, Xiao S, Chen QF. 2017. The AMP-activated protein kinase KIN10 is involved in the regulation of autophagy in Arabidopsis. Frontiers in Plant Science **8**, 1201.

Chresta CM, Davies BR, Hickson I, *et al*. 2010. AZD8055 is a potent, selective, and orally bioavailable ATP-competitive mammalian target of rapamycin kinase inhibitor with in vitro and in vivo antitumor activity. Cancer Research **70**, 288–298.

Christopherson RI, Lyons SD, Wilson PK. 2002. Inhibitors of de novo nucleotide biosynthesis as drugs. Accounts of Chemical Research **35**, 961–971.

Chung SC, Rédei GP. 1974. An anomaly of the genetic regulation of the de novo pyrimidine pathway in the plant Arabidopsis. Biochemical Genetics **11**, 441–453.

Chung T, Phillips AR, Vierstra RD. 2010. ATG8 lipidation and ATG8-mediated autophagy in Arabidopsis require ATG12 expressed from the differentially controlled ATG12A and ATG12B loci. The Plant Journal **62**, 483–493.

Contento AL, Xiong Y, Bassham DC. 2005. Visualization of autophagy in Arabidopsis using the fluorescent dye monodansylcadaverine and a GFP–AtATG8e fusion protein. The Plant Journal **42**, 598–608.

Córdoba-Cañero D, Dubois E, Ariza RR, Doutriaux MP, Roldán-Arjona T. 2010. Arabidopsis uracil DNA glycosylase (UNG) is required for base excision repair of uracil and increases plant sensitivity to 5-fluorouracil. Journal of Biological Chemistry **285**, 7475–7483.

Deprost D, Truong HN, Robaglia C, Meyer C. 2005. An Arabidopsis homolog of RAPTOR/KOG1 is essential for early embryo development. Biochemical and Biophysical Research Communications **326**, 844–850.

Dettmer J, Hong-Hermesdorf A, Stierhof YD, Schumacher K. 2006. Vacuolar H^+-ATPase activity is required for endocytic and secretory trafficking in Arabidopsis. The Plant Cell **18**, 715–730.

Dobrenel T, Caldana C, Hanson J, Robaglia C, Vincentz M, Veit B, Meyer C. 2016. TOR signaling and nutrient sensing. Annual Review of Plant Biology **67**, 261–285.

Doelling JH, Walker JM, Friedman EM, Thompson AR, Vierstra RD. 2002. The APG8/12-activating enzyme APG7 is required for proper nutrient recycling and senescence in *Arabidopsis thaliana*. Journal of Biological Chemistry **277**, 33105–33114.

Doerner P. 2007. Signals and mechanisms in the control of plant growth. In: Bögre L, Beemster G, eds. Plant growth signaling. Plant cell monographs, Vol. **10**. Berlin, Heidelberg: Springer, 1–23.

Dong Y, Teleman AA, Jedmowski C, Wirtz M, Hell R. 2019. The Arabidopsis THADA homologue modulates TOR activity and cold acclimation. Plant Biology **21** Suppl 1, 77–83.

Dröse S, Bindseil KU, Bowman EJ, Siebers A, Zeeck A, Altendorf K. 1993. Inhibitory effect of modified bafilomycins and concanamycins on P- and V-type adenosinetriphosphatases. Biochemistry **32**, 3902–3906.

Emmanuel N, Ragunathan S, Shan Q, Wang F, Giannakou A, Huser N, Jin G, Myers J, Abraham RT, Unsal-Kacmaz K. 2017. Purine nucleotide availability regulates mTORC1 activity through the Rheb GTPase. Cell Reports **19**, 2665–2680.

Fennoy SL, Jayachandran S, Bailey-Serres J. 1997. RNase activities are reduced concomitantly with conservation of total cellular RNA and ribosomes in O_2-deprived seedling roots of maize. Plant Physiology **115**, 1109–1117.

Floyd BE, Morriss SC, MacIntosh GC, Bassham DC. 2015. Evidence for autophagy-dependent pathways of rRNA turnover in Arabidopsis. Autophagy **11**, 2199–2212.

Floyd BE, Mugume Y, Morriss SC, MacIntosh GC, Bassham DC. 2017. Localization of RNS2 ribonuclease to the vacuole is required for its role in cellular homeostasis. Planta **245**, 779–792.

Girke C, Daumann M, Niopek-Witz S, Möhlmann T. 2014. Nucleobase and nucleoside transport and integration into plant metabolism. Frontiers in Plant Science **5**, 443.

Hanaoka H, Noda T, Shirano Y, Kato T, Hayashi H, Shibata D, Tabata S, Ohsumi Y. 2002. Leaf senescence and starvation-induced chlorosis are accelerated by the disruption of an Arabidopsis autophagy gene. Plant Physiology **129**, 1181–1193.

Hara K, Maruki Y, Long X, Yoshino K, Oshiro N, Hidayat S, Tokunaga C, Avruch J, Yonezawa K. 2002. Raptor, a binding partner of target of rapamycin (TOR), mediates TOR action. Cell **110**, 177–189.

Hardie DG. 2011. AMP-activated protein kinase: an energy sensor that regulates all aspects of cell function. Genes & Development **25**, 1895–1908.

Haud N, Kara F, Diekmann S, *et al.* 2011. rnaset2 mutant zebrafish model familial cystic leukoencephalopathy and reveal a role for RNase T2 in degrading ribosomal RNA. Proceedings of the National Academy of Sciences, USA **108**, 1099–1103.

Henneke M, Diekmann S, Ohlenbusch A, *et al.* 2009. RNASET2-deficient cystic leukoencephalopathy resembles congenital cytomegalovirus brain infection. Nature Genetics **41**, 773–775.

Hillwig MS, Contento AL, Meyer A, Ebany D, Bassham DC, Macintosh GC. 2011. RNS2, a conserved member of the RNase T2 family, is necessary for ribosomal RNA decay in plants. Proceedings of the National Academy of Sciences, USA **108**, 1093–1098.

Houseley J, Tollervey D. 2009. The many pathways of RNA degradation. Cell **136**, 763–776.

Hoxhaj G, Hughes-Hallett J, Timson RC, Ilagan E, Yuan M, Asara JM, Ben-Sahra I, Manning BD. 2017. The mTORC1 signaling network senses changes in cellular purine nucleotide levels. Cell Reports **21**, 1331–1346.

Huang H, Kawamata T, Horie T, Tsugawa H, Nakayama Y, Ohsumi Y, Fukusaki E. 2015. Bulk RNA degradation by nitrogen starvation-induced autophagy in yeast. The EMBO Journal **34**, 154–168.

Huss M, Ingenhorst G, König S, Gassel M, Dröse S, Zeeck A, Altendorf K, Wieczorek H. 2002. Concanamycin A, the specific inhibitor of V-ATPases, binds to the V(o) subunit c. Journal of Biological Chemistry **277**, 40544–40548.

Iadevaia V, Liu R, Proud CG. 2014. mTORC1 signaling controls multiple steps in ribosome biogenesis. Seminars in Cell & Developmental Biology **36**, 113–120.

Izumi M, Ishida H, Nakamura S, Hidema J. 2017. Entire photodamaged chloroplasts are transported to the central vacuole by autophagy. The Plant Cell **29**, 377–394.

Kazibwe Z, Liu AY, MacIntosh GC, Bassham DC. 2019. The ins and outs of autophagic ribosome turnover. Cells **8**, 1603.

Kemper E, Grevelding C, Schell J, Masterson R. 1992. Improved method for the transformation of *Arabidopsis thaliana* with chimeric dihydrofolate reductase constructs which confer methotrexate resistance. Plant Cell Reports **11**, 118–121.

Kirisako T, Baba M, Ishihara N, Miyazawa K, Ohsumi M, Yoshimori T, Noda T, Ohsumi Y. 1999. Formation process of autophagosome is traced with Apg8/Aut7p in yeast. Journal of Cell Biology **147**, 435–446.

Klionsky DJ, Abdelmohsen K, Abe A, *et al.* 2016. Guidelines for the use and interpretation of assays for monitoring autophagy (3rd edition). Autophagy **12**, 1–222.

Kraft C, Deplazes A, Sohrmann M, Peter M. 2008. Mature ribosomes are selectively degraded upon starvation by an autophagy pathway requiring the Ubp3p/Bre5p ubiquitin protease. Nature Cell Biology **10**, 602–610.

Lafontaine DL. 2010. A 'garbage can' for ribosomes: how eukaryotes degrade their ribosomes. Trends in Biochemical Sciences **35**, 267–277.

Lee JW, Park S, Takahashi Y, Wang HG. 2010. The association of AMPK with ULK1 regulates autophagy. PLoS One **5**, e15394.

Li F, Chung T, Vierstra RD. 2014. AUTOPHAGY-RELATED11 plays a critical role in general autophagy- and senescence-induced mitophagy in Arabidopsis. The Plant Cell **26**, 788–807.

Li F, Vierstra RD. 2012. Autophagy: a multifaceted intracellular system for bulk and selective recycling. Trends in Plant Science **17**, 526–537.

Li L, Song Y, Wang K, Dong P, Zhang X, Li F, Li Z, Ren M. 2015. TOR-inhibitor insensitive-1 (TRIN1) regulates cotyledons greening in Arabidopsis. Frontiers in Plant Science **6**, 861.

Li X, Cai W, Liu Y, Li H, Fu L, Liu Z, Xu L, Liu H, Xu T, Xiong Y. 2017. Differential TOR activation and cell proliferation in Arabidopsis root and shoot apexes. Proceedings of the National Academy of Sciences, USA **114**, 2765–2770.

Liao XH, Majithia A, Huang X, Kimmel AR. 2008. Growth control via TOR kinase signaling, an intracellular sensor of amino acid and energy availability, with crosstalk potential to proline metabolism. Amino Acids **35**, 761–770.

Liu Y, Bassham DC. 2010. TOR is a negative regulator of autophagy in *Arabidopsis thaliana*. PLoS One **5**, e11883.

Liu Y, Bassham DC. 2012. Autophagy: pathways for self-eating in plant cells. Annual Review of Plant Biology **63**, 215–237.

Liu Y, Burgos JS, Deng Y, Srivastava R, Howell SH, Bassham DC. 2012. Degradation of the endoplasmic reticulum by autophagy during endoplasmic reticulum stress in Arabidopsis. The Plant Cell **24**, 4635–4651.

Liu Y, Xiong Y, Bassham DC. 2009. Autophagy is required for tolerance of drought and salt stress in plants. Autophagy **5**, 954–963.

Liu YB, Zou W, Yang PG, Wang L, Ma Y, Zhang H, Wang XC. 2018. Autophagy-dependent ribosomal RNA degradation is essential for maintaining nucleotide homeostasis during *C. elegans* development. eLife **7**, e36588.

Loizeau K, De Brouwer V, Gambonnet B, Yu A, Renou JP, Van Der Straeten D, Lambert WE, Rébeillé F, Ravanel S. 2008. A genome-wide and metabolic analysis determined the adaptive response of Arabidopsis cells to folate depletion induced by methotrexate. Plant Physiology **148**, 2083–2095.

Margalha L, Confraria A, Baena-González E. 2019. SnRK1 and TOR: modulating growth–defense trade-offs in plant stress responses. Journal of Experimental Botany **70**, 2261–2274.

Meyer R, Wagner KG. 1985. Determination of nucleotide pools in plant tissue by high-performance liquid chromatography. Analytical Biochemistry **148**, 269–276.

Moffatt BA, Ashihara H. 2002. Purine and pyrimidine nucleotide synthesis and metabolism. The Arabidopsis Book **1**, e0018.

Moffatt B, Somerville C. 1988. Positive selection for male-sterile mutants of Arabidopsis lacking adenine phosphoribosyl transferase activity. Plant Physiology **86**, 1150–1154.

Moreau M, Azzopardi M, Clément G, *et al.* 2012. Mutations in the Arabidopsis homolog of LST8/GβL, a partner of the target of Rapamycin kinase, impair plant growth, flowering, and metabolic adaptation to long days. The Plant Cell **24**, 463–481.

Morriss SC, Liu X, Floyd BE, Bassham DC, MacIntosh GC. 2017. Cell growth and homeostasis are disrupted in arabidopsis *rns2-2* mutants missing the main vacuolar RNase activity. Annals of Botany **120**, 911–922.

Pérez-Pérez ME, Florencio FJ, Crespo JL. 2010. Inhibition of target of rapamycin signaling and stress activate autophagy in *Chlamydomonas reinhardtii*. Plant Physiology **152**, 1874–1888.

Pu Y, Luo X, Bassham DC. 2017. TOR-dependent and -independent pathways regulate autophagy in *Arabidopsis thaliana*. Frontiers in Plant Science **8**, 1204.

Robitaille AM, Christen S, Shimobayashi M, Cornu M, Fava LL, Moes S, Prescianotto-Baschong C, Sauer U, Jenoe P, Hall MN. 2013. Quantitative phosphoproteomics reveal mTORC1 activates de novo pyrimidine synthesis. Science **339**, 1320–1323.

Schaeffer GW, Sorokin T. 1966. Growth inhibition of tobacco tissue cultures with 6-azauracil, 6-azauridine and maleic hydrazide. Plant Physiology **41**, 971–975.

Schepetilnikov M, Dimitrova M, Mancera-Martínez E, Geldreich A, Keller M, Ryabova LA. 2013. TOR and S6K1 promote translation reinitiation of uORF-containing mRNAs via phosphorylation of eIF3h. The EMBO Journal **32**, 1087–1102.

Schepetilnikov M, Makarian J, Srour O, Geldreich A, Yang Z, Chicher J, Hammann P, Ryabova LA. 2017. GTPase ROP2 binds and promotes activation of target of rapamycin, TOR, in response to auxin. The EMBO Journal **36**, 886–903.

Schneider CA, Rasband WS, Eliceiri KW. 2012. NIH image to ImageJ: 25 years of image analysis. Nature Methods **9**, 671–675.

Shin KD, Lee HN, Chung T. 2014. A revised assay for monitoring autophagic flux in *Arabidopsis thaliana* reveals involvement of AUTOPHAGY-RELATED9 in autophagy. Molecules and Cells **37**, 399–405.

Shull TE, Kurepa J, Smalle JA. 2019. Anatase TiO2 nanoparticles induce autophagy and chloroplast degradation in thale cress (*Arabidopsis thaliana*). Environmental Science & Technology **53**, 9522–9532.

Slobodkin MR, Elazar Z. 2013. The Atg8 family: multifunctional ubiquitin-like key regulators of autophagy. Essays in Biochemistry **55**, 51–64.

Soto-Burgos J, Bassham DC. 2017. SnRK1 activates autophagy via the TOR signaling pathway in *Arabidopsis thaliana*. PLoS One **12**, e0182591.

Stasolla C, Loukanina N, Ashihara H, Yeung EC, Thorpe TA. 2006. Changes of purine and pyrimidine nucleotide biosynthesis during shoot initiation from epicotyl explants of white spruce (*Picea glauca*). Plant Science **171**, 345–354.

Suttangkakul A, Li F, Chung T, Vierstra RD. 2011. The ATG1/ATG13 protein kinase complex is both a regulator and a target of autophagic recycling in Arabidopsis. The Plant Cell **23**, 3761–3779.

Taylor CB, Bariola PA, delCardayré SB, Raines RT, Green PJ. 1993. RNS2: a senescence-associated RNase of Arabidopsis that diverged from the S-RNases before speciation. Proceedings of the National Academy of Sciences, USA **90**, 5118–5122.

Thompson AR, Doelling JH, Suttangkakul A, Vierstra RD. 2005. Autophagic nutrient recycling in Arabidopsis directed by the ATG8 and ATG12 conjugation pathways. Plant Physiology **138**, 2097–2110.

Turck F, Zilbermann F, Kozma SC, Thomas G, Nagy F. 2004. Phytohormones participate in an S6 kinase signal transduction pathway in Arabidopsis. Plant Physiology **134**, 1527–1535.

Valvezan AJ, Turner M, Belaid A, *et al.* 2017. mTORC1 couples nucleotide synthesis to nucleotide demand resulting in a targetable metabolic vulnerability. Cancer Cell **32**, 624–638.

Van Leene J, Han C, Gadeyne A, *et al.* 2019. Capturing the phosphorylation and protein interaction landscape of the plant TOR kinase. Nature Plants **5**, 316–327.

Wang P, Mugume Y, Bassham DC. 2018. New advances in autophagy in plants: regulation, selectivity and function. Seminars in Cell & Developmental Biology **80**, 113–122.

Wang Z, Wilson WA, Fujino MA, Roach PJ. 2001. Antagonistic controls of autophagy and glycogen accumulation by Snf1p, the yeast homolog of AMP-activated protein kinase, and the cyclin-dependent kinase Pho85p. Molecular and Cellular Biology **21**, 5742–5752.

Warner JR. 1999. The economics of ribosome biosynthesis in yeast. Trends in Biochemical Sciences **24**, 437–440.

Xiong Y, Contento AL, Nguyen PQ, Bassham DC. 2007. Degradation of oxidized proteins by autophagy during oxidative stress in Arabidopsis. Plant Physiology **143**, 291–299.

Xiong Y, McCormack M, Li L, Hall Q, Xiang C, Sheen J. 2013. Glucose–TOR signalling reprograms the transcriptome and activates meristems. Nature **496**, 181–186.

Xiong Y, Sheen J. 2012. Rapamycin and glucose–target of rapamycin (TOR) protein signaling in plants. Journal of Biological Chemistry **287**, 2836–2842.

Yoshimoto K, Hanaoka H, Sato S, Kato T, Tabata S, Noda T, Ohsumi Y. 2004. Processing of ATG8s, ubiquitin-like proteins, and their deconjugation by ATG4s are essential for plant autophagy. The Plant Cell **16**, 2967–2983.

Zhang Y, Primavesi LF, Jhurreea D, Andralojc PJ, Mitchell RA, Powers SJ, Schluepmann H, Delatte T, Wingler A, Paul MJ. 2009. Inhibition of SNF1-related protein kinase1 activity and regulation of metabolic pathways by trehalose-6-phosphate. Plant Physiology **149**, 1860–1871.

Zrenner R, Stitt M, Sonnewald U, Boldt R. 2006. Pyrimidine and purine biosynthesis and degradation in plants. Annual Review of Plant Biology **57**, 805–836.